International Journal of Applied Pharmaceutics

ISSN- 0975-7058 Vol 15, Issue 1, 2023

Original Article

FORMULATION AND *IN VITRO* CHARACTERISATION OF GLUCOSE-RESPONSIVE NANOCAPSULES FOR THE DELIVERY OF M-INSULIN

NIKHAR VISHWAKARMA[1], SURESH P. VYAS[1*]

[1]Drug Delivery Research Laboratory, Department of Pharmaceutical Sciences, Dr Harisingh Gour University Sagar, M. P. 470003. India
Email: 01nikhar@gmail.com

Received: 05 Oct 2022, Revised and Accepted: 22 Oct 2022

ABSTRACT

Objective: The present study aimed to develop and characterize Chitosan coated Alginate Nanocapsules loaded with M-Insulin Concanavalin A Complex for glucose-responsive delivery.

Methods: Preformulation studies were performed on the Insulin human recombinant and the Nanocapsules were prepared by the ionic gelation method and coated with chitosan using electrostatic attraction. The formulation variables were optimized using Box-Behnken design (BBD) with the help of Design-Expert® Software. Three independent variables taken were the concentration of chitosan (A_1), the concentration of sodium alginate (A_2), and the stirring rate (A_3). The response variables selected were the average particle size (nm) (B_1), polydispersity index (B_2), and cumulative release (%) (B_3).

Results: The results from the Preformulation studies indicated that the received sample of the Insulin human recombinant was pure. The optimized nanocapsules possessed an average particle size of 382.4 nm, PDI 0.211 and zeta potential of 30.25 mV. The entrapment efficiency was found to be 79.2 %. The nanocapsules were further characterized for their surface morphology using TEM and were found to be of regular shape. The *in vitro* drug release study indicated that the nanocapsules were able to release 58 % of M-insulin in hyperglycaemic conditions for 12 h.

Conclusion: The outcomes of the study demonstrated that the developed nanocapsules can be effectively used for glucose-responsive delivery of M-insulin.

Keywords: Diabetes, Insulin, Nanocapsules, Glucose-responsive

DOI: https://dx.doi.org/10.22159/ijap.2023v15i1.46511. Journal homepage: https://innovareacademics.in/journals/index.php/ijap

INTRODUCTION

Type I Diabetes Mellitus (T1DM), also known as Insulin-dependent diabetes mellitus, is a metabolic disease caused by the inability to produce Insulin within the body leading to hyperglycemia [1]. T1DM and the associated secondary complications such as neuropathy [2], retinopathy [3], nephropathy [4], and cardiovascular diseases [5] are the major causes of mortality. T1DM and its associated complications have caused 4.2 million deaths in 2019 [6] and 6.7 million deaths in 2021 [7]. The casualties with T1DM and its associated secondary complications are expected to increase exponentially in the upcoming years. The current treatment for patients suffering from T1DM involves glucose measurements and insulin injections multiple times a day [8]. Many types of insulins, such as long-acting, intermediate-acting, short-acting and rapidly-acting, are already available [9–12]. The regular administration of insulin to patients is not only painful and inconvenient, but the fluctuations in the glycemic levels also lead to the development of secondary diabetes-associated complications. Despite the regular insulin injection, sufficient maintenance of blood glucose levels in the normoglycemic range is yet to be achieved. Thus, a glucose-responsive system that can release insulin based on the glucose concentration in the blood has the potential to improvise the current diabetic treatment. Various approaches have been attempted in the past such as the development of insulin infusion pumps [13–15]; however, many challenges, including the lack of signal and inadequacy in the detection of glucose levels are yet to be addressed [16].

Different approaches for the glucose-responsive release of insulin have already been reported by researchers. Such systems were based on phenylboronic acid (PBA) [17], a plant lectin (Concanavalin A) [18] and pH-responsive systems based on enzyme (Glucose oxidase) [19, 20]. Since Concanavalin A has an affinity toward glucose, it can be utilized for the fabrication of the glucose-responsive nanosystem. To overcome the shortcomings of current therapy, we have developed a glucose-responsive nanosystem that can release Maltose insulin in response to glucose levels. The nanosystem (nanocapsules) is based on encapsulating derivatized insulin (Maltose insulin) bound to the concanavalin A which has a well-reported affinity for glucose. Box-Behnken Design (BBD) is used for the efficient optimization of the formulation variables. The Maltose insulin Concanavalin A complex was encapsulated within the nanocapsules prepared by sodium alginate and chitosan to achieve the desired glucose-responsive delivery for the treatment of diabetes mellitus.

MATERIALS AND METHODS

Materials

Insulin Human Recombinant and Low molecular weight Chitosan were procured from Sigma Aldrich, United Kingdom, Sodium Alginate was purchased from Central Drug House (P) Ltd., New Delhi, India. Calcium chloride (fused) and Buffer tablets pH 7.4 were purchased from Loba Chemie Laboratory Reagents and Fine Chemicals, Thane, India. D-Glucose was purchased from Qualigens Fine Chemicals, Mumbai, India. Dialysis tubing (Molecular weight cut off 12000-14000 Dalton) was obtained from Himedia Laboratories, Mumbai, India. All other reagents used during the experiments were of analytical grade.

Preformulation studies

Preformulation studies are defined as the preliminary process of determining the physicochemical properties of the drug and the excipients, which are crucial for the preparation of the effective, safe and highly stable dosage form [21]. These studies are carried out to determine the optimum conditions for the preparation of dosage forms with desired characteristics.

Physical properties

The physical attributes of the Insulin human recombinant such as colour, nature and odour were examined in broad daylight.

Partition coefficient

Briefly, 10 mg of Insulin human recombinant was accurately weighed and poured into a volumetric flask containing 10 ml of n-Octanol (organic phase) and 10 ml of PBS pH 7.4t (aqueous phase). The volumetric flask containing the immiscible phases with the

Insulin was placed on an orbital shaker for 24 h at ambient room temperature. After the completion of 24 h both the phases i.e., organic and aqueous phases were separated using the separating funnel [21]. The concentration of the Insulin was determined in the aqueous phase using the UV Visible Spectrophotometer (Orion Aquamate 8000, Thermo Fisher Scientific, USA) at λ_{max} 276 nm. The partition coefficient was calculated using the formula:

$$\text{Partition coefficient} = \frac{\text{Concentration of drug in organic phase } (C_{org.})}{\text{Concentration of drug in aqueous phase } (C_{aq.})} \text{ at Equilibrium}$$

Solubility studies

The solubility of Insulin human recombinant was determined in various aqueous and non-aqueous solvents [22] such as distilled water, 0.01 M HCl, PBS pH 7.4, ethanol, and chloroform and recorded in table 1.

UV spectroscopy

The UV spectrum of Insulin human recombinant was obtained using the UV Visible Spectrometer (Orion Aquamate 8000, Thermo Fisher Scientific, USA). Accurately weighed 10 mg of Insulin human recombinant was taken in a volumetric flask and dissolved in a minimum quantity of PBS pH 7.4; finally, the volume was made up to 10 ml using PBS pH 7.4. Approximately, 3 ml of a clear solution of Insulin human recombinant in PBS pH 7.4 was taken in a quartz cuvette and kept in the sample holder of a UV spectrophotometer. The absorbance was measured in the photometric mode in the scanning range from 200 to 400 nm and the λ_{max} was determined [23].

FTIR spectroscopy

FTIR Spectrum of the Insulin Human Recombinant was obtained using FTIR Spectrophotometer (Agilent Cary 630 FTIR spectrometer, CA USA). A small amount of Insulin Human Recombinant was placed onto the top of the sample holder and pressed using the knob. The drug was then analyzed using the Agilent microlabs PC software to obtain the IR Spectrum [24].

Quantitative estimation

The Insulin human recombinant was estimated by UV absorption using a spectrophotometer. Accurately weighed 10 mg of Insulin Human Recombinant was taken in a volumetric flask and the volume was made up to 10 ml using phosphate buffer pH 7.4. Aliquots of volume 0.1-1.0 ml were carefully pipetted out from the stock solution and the volume was made up to 10 ml using phosphate buffer pH 7.4 to prepare the sub-stock solutions of concentrations ranging from 100 to 1000 µg/ml [25]. The aliquots were then analyzed using UV Visible spectrophotometer (Orion Aquamate 8000, Thermo Fisher Scientific, USA) and the absorbance values were measured at wavelength maxima 276 nm against the blank. The calibration curve was constructed by plotting the absorbance against concentration.

Preparation, optimization and characterization of chitosan-coated alginate nanocapsules loaded with M-insulin con A complex (CANCs)

Preparation of CANCs

The Maltose Insulin was synthesized using the method reported in the literature [26] and was complexed with Concanavalin A [27]. The alginate nanocapsules were prepared using the ionic gelation method reported by Shen *et al.*, [28]. Briefly, 1 % w/v sodium alginate dissolved in 10 mmol HEPES buffer (pH 7.4) and 20 mmol calcium chloride were used to form the alginate nanocapsules. 5 mg of M-Insulin Con A complex was incorporated in the alginate solution before the formulation of nanocapsules. The obtained M-insulin Con A complex loaded alginate nanocapsules were coated using Chitosan. The coating solution was prepared by dissolving 0.5 % w/v low molecular weight Chitosan in 1 % v/v acetic acid. The pH of the coating solution and alginate nanocapsules suspension was adjusted to 4.6 and 4.9, respectively [29]. The coating solution was then added dropwise in the alginate nanocapsules suspension and stirred for 30 min at 1000 RPM. The prepared CANCs were then centrifuged for 30 min at 10000 RPM and 4 °C using the ultra-centrifuge (Z36 HK, Hermle Labortechnik, Germany). Different formulation variables such as Chitosan concentration, Alginate concentration and stirring rate were optimized to obtain CANCs with minimum average particle size, low polydispersity index and maximum cumulative release.

Optimization of variables

The process variables used in the preparation of nanocapsules were optimized using the Response Surface Model (RSM) approach using a 3-factor, 3-level Box-Behnken design (BBD) [30]. The RSM was utilized to study the impact of independent variables on the dependent variables for the optimization of the nanocapsules. The three factors or independent variables considered for the study were the concentration of Chitosan (0.5 %, 1.0 % and 1.5 %) (A_1), the concentration of sodium alginate (0.8 %, 1.0 % and 1.2 %) (A_2) and the stirring rate (900, 1000 and 1100 RPM) (A_3). The Average Particle Size (B_1), Polydispersity index (B_2), and Cumulative Release (B_3) were the dependent variables or chosen responses.

Characterization of optimized CANCs

The prepared optimized CANCs were characterized for various parameters, including average particle size, polydispersity index and zeta potential through photon correlation spectroscopy (Zetasizer Nano-ZS90 instrument, Malvern, UK); the shape and surface morphology of the optimized CANCs were determined by using transmission electron microscopy (TEM-FEI Technai G2 12 Biotwin, FEI Company, USA).

Percentage entrapment efficiency

The percentage entrapment efficiency of the optimized CANCs was determined by an indirect method [31]. The suspension of CANCs was centrifuged at 15000 RPM for 10 min using the ultracentrifuge (Z36 HK, Hermle Labortechnik, Germany) and the supernatant was separated and filtered using a 0.22 µm filter. The supernatant was then analyzed for the M-Insulin content by measuring the absorbance at 276 nm using the UV Visible spectrophotometer (Orion Aquamate 8000, Thermo Fisher Scientific, USA). The percentage entrapment efficiency was determined using the formula:

$$\% \text{ Entrapment efficiency} = \frac{\text{Total amount of M Insulin added} - \text{Amount of M Insulin in supernatent}}{\text{Total amount of M Insulin added}} X100$$

***In vitro* release study**

The *in vitro* release of maltose insulin (M-Insulin) from the chitosan-coated alginate nanocapsules (CANCs) was studied in glucose mediums with different molar concentrations [18]. The M-Insulin-Con A complex loaded CANCs suspension was kept in a dialysis bag (MWCO 12000-14000, Himedia Laboratories, India). The dialysis was performed by placing the dialysis bags in glucose mediums with different molar concentrations of 2.77 mmol/l (hypoglycemic condition), 5.55 mmol/l (normoglycemic condition) and 11.1 mmol/l (hyperglycemic condition). The samples were withdrawn at regular intervals and the sink condition was maintained during the process. The dialysis was performed for 12 h in each medium at 37 °C with continuous stirring. The amount of M-insulin released in the medium was analyzed by UV Visible spectrophotometer (Orion Aquamate 8000, Thermo Fisher Scientific, USA) at λ_{max} 276 nm.

Statistical analysis

Design-Expert software (Version: 13.0.9.0 Stat-Ease, Inc., Minneapolis, USA) was used to perform the statistical optimization

RESULTS AND DISCUSSION

Preformulation studies

Insulin Human Recombinant was procured as white crystalline, odourless powder. The physical appearance, colour and nature were found to be in accordance with that reported in the literature. The partition coefficient of Insulin Human Recombinant was performed in n-Octanol and PBS (pH 7.4) and the log P value was found to be 0.827 suggesting the hydrophilic nature of the drug (table 1). The absorption maximum of the drug in PBS pH 7.4 was measured by UV

Visible spectrophotometer (Orion Aquamate 8000, Thermo Fisher Scientific, USA) and the characteristic absorbance was obtained at 276 nm (fig. 1A). The calibration curve of Insulin Human Recombinant was prepared in PBS pH 7.4 using the UV-Visible Spectrophotometer. The aliquots of concentrations ranging from 100 to 1000 µg/ml were made in PBS (pH 7.4) and analyzed at 276 nm. The graph showed linearity with a correlation coefficient value of 0.9997 and the equation of the line was Y = 0.001x − 0.0026 (fig. 1B). The FTIR spectrum of Insulin Human Recombinant has shown the presence of different characteristic groups (fig. 1C). The peaks in the FTIR spectrum were found to be in accordance with the reported literature [32] and confirmed the presence of desired functional groups peaks at 3283.7 for N-H stretching, 1640.02 for characteristic Amide-I (N-H Bending), 1513.2 for Amide-II (N-H), 1386.5 for C-N Stretching (aromatic amines) and 1233.7 for C-N Stretching (Aliphatic amines) (table 1). It can be concluded from the Preformulation studies that the procured drug i.e., Insulin Human Recombinant used in the present study was pure.

Table 1: Physical appearance, partition coefficient and solubility of Insulin human recombinant in various solvents

Physical properties	Experimental observation
Colour	White
Odour	Odourless
Nature	Crystalline
Medium	Partition Coefficient (O/W)
n-octanol: PBS (pH 7.4)	0.827
Solvent	Solubility
0.01M HCl	++++
PBS pH 7.4	++++
Distilled water	++
Chloroform	---
Ethanol	---
IR absorption band (cm^{-1})	Assignments
3283.7	N-H Stretching
1640.029	Amide I N-H bending
1513.299	Amide II (N-H)
1386.5	C-N Stretching (aromatic amines)
1233.749	C-N Stretching (aliphatic amines)

---Insoluble, ++++Freely soluble, ++soluble

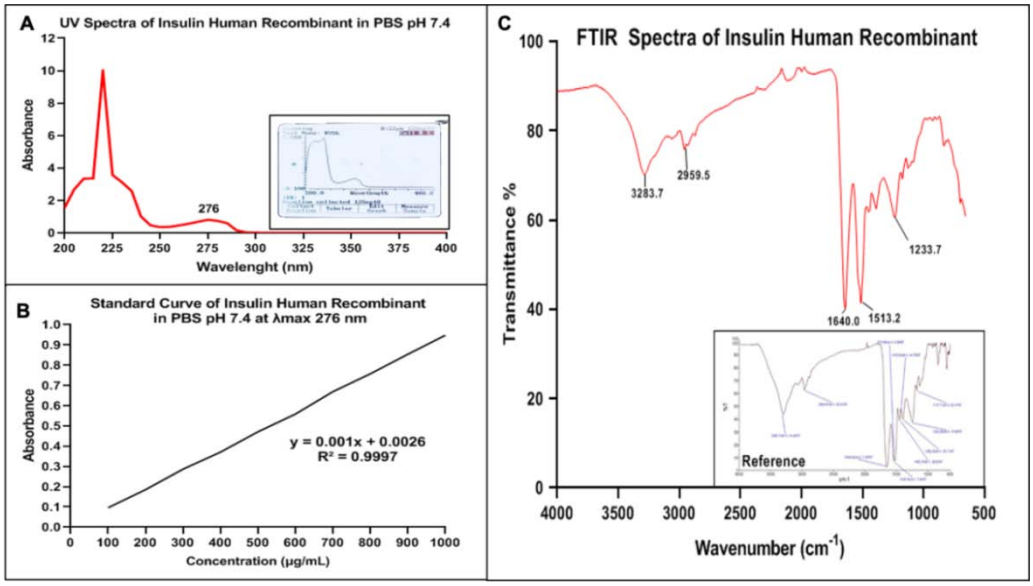

Fig. 1: A. UV spectrum of insulin human recombinant in PBS pH 7.4, B. Standard/Calibration curve of insulin human recombinant in PBS pH 7.4 at λ_{max} 276 nm, C. Comparison of IR Spectra of insulin human recombinant in reference and test sample

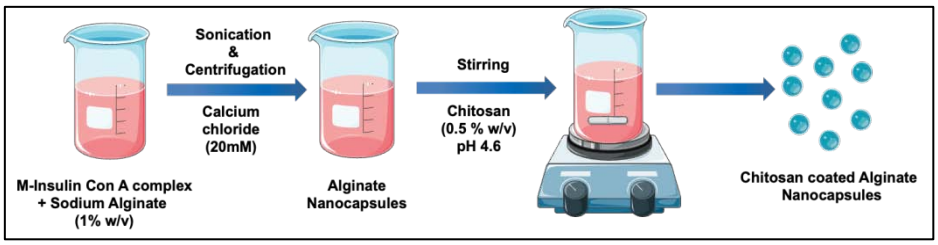

Fig. 2: Scheme for the preparation of Chitosan coated Alginate nanocapsules loaded with M-Insulin Con A complex

Preparation of chitosan-coated alginate nanocapsules loaded with M-insulin concanavalin a complex (CANCs)

The Maltose insulin was synthesized using the method reported in the literature [26]. The M-insulin was then bound to the lectin (Con A), which has a well-established affinity toward glucose [27]. The M-Insulin Con A complex obtained was incorporated into the Alginate nanocapsules [28] and then the capsules were coated using chitosan by the method reported by Bruno *et al.*, [29] (fig. 2).

Optimization of variables

Box-Behnken Design (BBD) was utilized to determine the optimum value of different independent variables (table 2). A total of 17 formulations of nanocapsules (CANC1-CANC17) were prepared and their 3D response curves were generated using Design-Expert software (Version: 13.0.9.0 Stat-Ease, Inc., Minneapolis, USA) (fig. 3).

The concentration of Chitosan (A_1) (%), the concentration of sodium alginate (%) (A_2) and stirring rate (RPM) (A_3) were used as dependent variables for the preparation and optimization of the Chitosan coated Alginate nanocapsules loaded with M-Insulin Con A complex. The optimization was carried out by keeping all the other variables constant.

The prepared CANCs were characterized for different parameters such as average particle size (nm), polydispersity index (PDI) and cumulative release (%). The responses obtained for different evaluation parameters are shown in table 3. The polynomial equation obtained from the experimental design is:

$$Y = \beta_0 + \beta_1 A_1 + \beta_2 A_2 + \beta_3 A_3 + \beta_4 A_1 A_2 + \beta_5 A_1 A_3 + \beta_6 A_2 A_3 + \beta_7 A_1^2 + \beta_8 A_2^2 + \beta_9 A_3^2 \ldots\ldots\ldots \text{Equation 1}$$

Table 2: Independent and dependent variables levels used in the box-behnken design

Factor independent variables	Levels used		
	-1	0	1
A_1 = Concentration of Chitosan (%)	0.5	1.0	1.5
A_2 = Concentration of Sodium Alginate (%)	0.8	1.0	1.2
A_3 = Stirring rate (RPM)	900	1000	1100
Dependent Variables	**Constraints**		
B_1 = Particle size (nm)	Minimize		
B_2 = Polydispersity index (PDI)	Less than 0.5		
B_3 = Cumulative release (%)	Maximum		

Table 3: Coding, composition and physicochemical properties of all prepared CANCs

Run	Formulation code	Factors (Independent variables)		Responses (Dependent variables)			
		Concentration of chitosan (%)	Concentration of sodium alginate (%)	Stirring rate (RPM)	Particle size (nm)	PDI	Cumulative release (%)
1	CANC1	1.5	0.8	1000	569.3	0.425	22
2	CANC2	1	1	1000	405.6	0.211	58
3	CANC3	0.5	0.8	1000	386.6	0.187	56
4	CANC4	1.5	1	900	643.5	0.543	37
5	CANC5	1.5	1.2	1000	647.5	0.641	21
6	CANC6	1	1	1000	414.1	0.199	55
7	CANC7	0.5	1	1100	389.3	0.147	58
8	CANC8	1	1	1000	410.7	0.216	57
9	CANC9	1	0.8	900	487.6	0.441	39
10	CANC10	1.5	1	1100	594.6	0.488	23
11	CANC11	1	1.2	1100	494.1	0.462	28
12	CANC12	1	1	1000	413.5	0.214	56
13	CANC13	1	1.2	900	489.8	0.486	27
14	CANC14	1	0.8	1100	419.6	0.358	32
15	CANC15	0.5	1.2	1000	382.4	0.157	42
16	CANC16	1	1	1000	409.7	0.197	55
17	CANC17	0.5	1	1000	382.4	0.211	58

All three responses (B_1, B_2 and B_3) generated for the model were found to have higher statistical significant values (P>0.0001). The responses obtained for R^2 values ranged between 0.9957 and 0.9989 indicating that the data generated by the polynomial equation (Equation 1) was an excellent fit. The lack of fit ranged from 0.1609 to 0.3191 for the generated models and was found to be not significant, demonstrating that the proposed model was suitable. The difference between adjusted $R^2$and the predicted R^2 for all the models was found to be less than 0.2 affirming the excellent fit of the models (table 4).

Table 4: Model summary and fit statistics for various dependent variables Average particle size (PS), Polydispersity index (PDI) and Cumulative release (CR)

Independent variable	Source	Sequential p-value	Lack of Fit p-value	Adjusted R^2	Predicted R^2	R^2
PS	Quadratic	<0.0001	0.1609	0.9975	0.9874	0.9989
PDI	Quadratic	<0.0001	0.2417	0.9955	0.9794	0.9980
CR	Quadratic	<0.0001	0.3191	0.9901	0.9589	0.9957

Impact of independent variables A_1, A_2 and A_3 on average particle size (B_1)

The quadratic equation 2 for the impact of independent variables on average particle size (B_1) is as follows:

$$\text{Average Particle Size } (B_1) = 410.72 + 114.28\,A_1 + 18.84\,A_2 - 13.21\,A_3 + 20.60\,A_1A_2 - 13.95\,A_1A_3 + 18.07\,A_2A_3 + 57.70\,A_1^2 + 28.03\,A_2^2 + 34.03\,A_3^2 \ldots\ldots\ldots \text{Equation 2.}$$

The average particle size of the prepared nanocapsules was found in the nanometric range (table 3) with the minimum particle size of 382.4 nm at 0.5 % w/v Chitosan concentration and increased to particle size was up to 647.5 nm on increasing the concentration to 1.5 % w/v. The increase in the particle size with an increase in chitosan concentration may be because of the ionotropic interactions [33] and also due to intramolecular hydrogen bonding between the positively charged chitosan at pH 4.6 and negatively charged carboxylic acid residues of the alginate nanocapsules [34](fig. 3A).

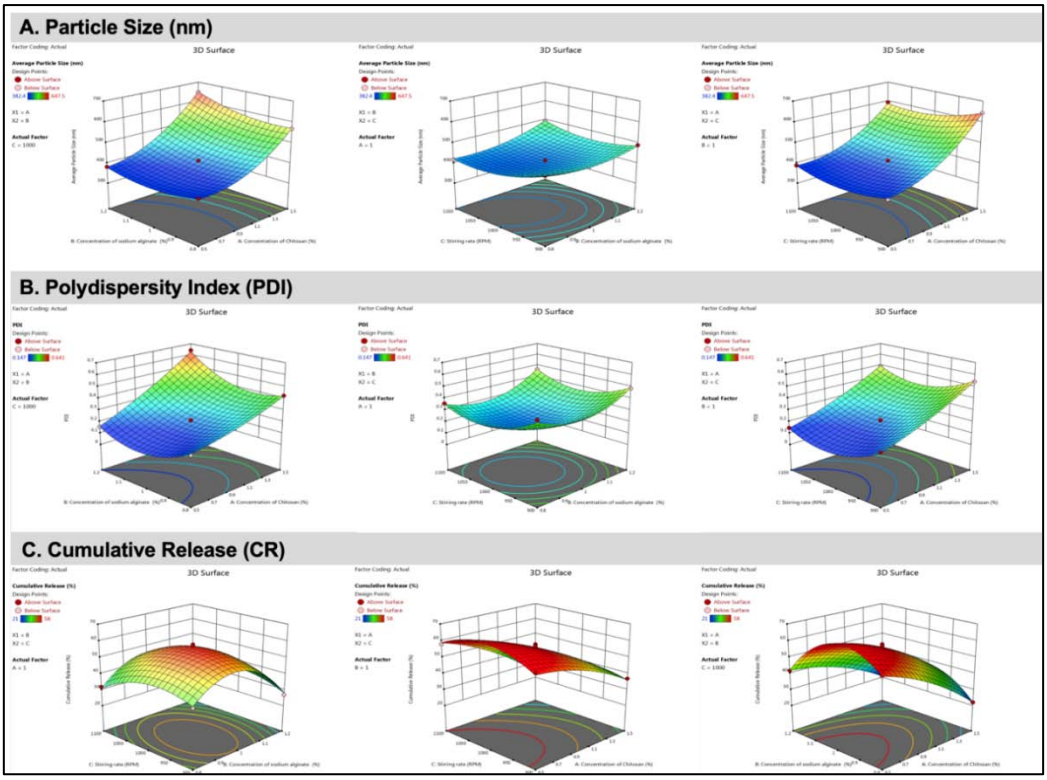

Fig. 3: 3D response curves obtained for the effects of various independent variables such as Chitosan concentration, Sodium alginate concentration and stirring rate on dependent variables such as A. Average particle size, B. Polydispersity index and C. Cumulative release (%)

Impact of independent variables A_1, A_2 and A_3 on polydispersity index (B_2)

The quadratic equation 3 for the impact of independent variables on the polydispersity index (B_2) is as follows:

$$\text{Polydispersity Index } (B_2) = 0.2074 + 0.1744\,A_1 + 0.0419\,A_2 - 0.0283\,A_3 + 0.0615\,A_1A_2 - 0.0023\,A_1A_3 + 0.0148\,A_2A_3 + 0.0278\,A_1^2 + 0.1173\,A_2^2 + 0.1121A_3^2 \quad \text{..... Equation 3}$$

The polydispersity index (PDI) was found in a relatively narrow range of distribution i.e., from 0.147 to 0.641. It was observed that the polydispersity index of the CANCs was increased with an increase in the chitosan concentration. This may be due to the formation of large aggregates of the CANCs due to the electrostatic attraction of chitosan with alginate nanocapsules. The result demonstrated that the low concentration of Chitosan produced CANCs with narrow size distribution [34] (fig. 3B).

Impact of independent variables A_1, A_2 and A_3 on cumulative release (%) (B_3)

The quadratic equation 4 for the impact of independent variables on cumulative release (%) (B_3) is as follows:

$$\text{Cumulative Release } (B_3) = 56.20 - 13.87\,A_1 - 3.87\,A_2 - 2.50\,A_3 + 3.25\,A_1A_2 - 3.50\,A_1A_3 + 2.00\,A_2A_3 - 4.23\,A_1^2 - 16.73A_2^2 - 7.97A_3^2 \quad \text{..... Equation 4}$$

It was evident from the above quadratic equation 4 that the impact of chitosan concentration (A_1) on the cumulative release of the M-insulin was significantly higher as compared to the other two factors. The cumulative release of M-insulin from the CANCs was found in the range of 21% to 58%. The chitosan concentration (A_1) has a significant impact on the cumulative release of the M-insulin from the CANCs (fig. 3C). The cumulative release from the prepared CANCs decreased with an increase in the chitosan concentration which can be ascribed to the decrease in the contact surface due to the production of large size CANCs with low surface area. Another probable reason for the decrease in the cumulative release with an increase in the chitosan concentration may be due to the deposition of the thick layer of chitosan polymer onto the surface of the alginate resulting in the narrowing of the pores and formation of additional polymeric barrier thicker than calcium alginate-based membrane [35].

The design of expert software suggested total of 3 solutions for the CANCs with the desirability value of 1.000, indicating the high predictability and robustness of the developed model. Optimized nanocapsules were selected based on maximum desirability with minimum average particle size and distribution (polydispersity index) and maximum cumulative release. The concentration of chitosan (A_1) (0.554 % w/v), the concentration of sodium alginate (A_2) (0.907 % w/v) and stirring rate (A_3) (974.753 RPM) were the components of the suggested composition of optimised CANCs (table 5). Out of the seventeen CANCs prepared, the experimental result of the formulation CANC17 was found to be near the predicted values of the responses. The predicted values for the average particle size (B_1), polydispersity index (B_2), and cumulative release (B_3) were 364.973 nm, PDI 0.122 and 64.334 % and the observed values corresponding to the average particle size (B_1), polydispersity index (B_2) and cumulative release (B_3) were 382.4 nm, 0.211 and 58.0 %, respectively. Thus, the CANC17 was selected as an optimized formulation for further characterization.

Table 5: Suggested solutions for the selection of optimized CANCs with desired responses

Number	A_1	A_2	A_3	B_1	B_2	B_3	Desirability	
1	0.554	0.907	974.753	364.973	0.122	64.334	1.000	Selected
2	0.526	0.976	1072.593	371.107	0.106	62.366	0.526	
3	0.556	0.981	1074.074	371.723	0.115	61.625	0.556	

The optimized nanocapsules (CANC17) formulation was then characterized for average particle size and zeta potential using the dynamic light scattering method (fig. 4A). The shape and surface morphology of the prepared CANCs were evaluated using Transmission Electron Microscopy (TEM).

The TEM study indicated that the prepared CANCs were of regular shape with a smooth surface and the diameter of the nanocapsules corroborates with the findings of the DLS measurement (fig. 4B). The chitosan-coated alginate nanocapsules were prepared by interaction of the positively charged chitosan (pka ~6.3) at pH 4.6 with the negatively charged alginate nanocapsules [29]. The result from the DLS measurement demonstrated that the zeta potential of alginate nanocapsules changed from-25.72 mV to 30.25 mV (fig. 4C and 4D). This inversion of charge from negative to positive indicated the interaction of chitosan with the alginate nanocapsules and the formation of an intact chitosan coat on alginate nanocapsules (CANCs). The entrapment efficiency of the CANCs was evaluated using the indirect method and was observed to be 79.2 %. No leakage of M-insulin was observed during the coating process of the chitosan on the alginate nanocapsules.

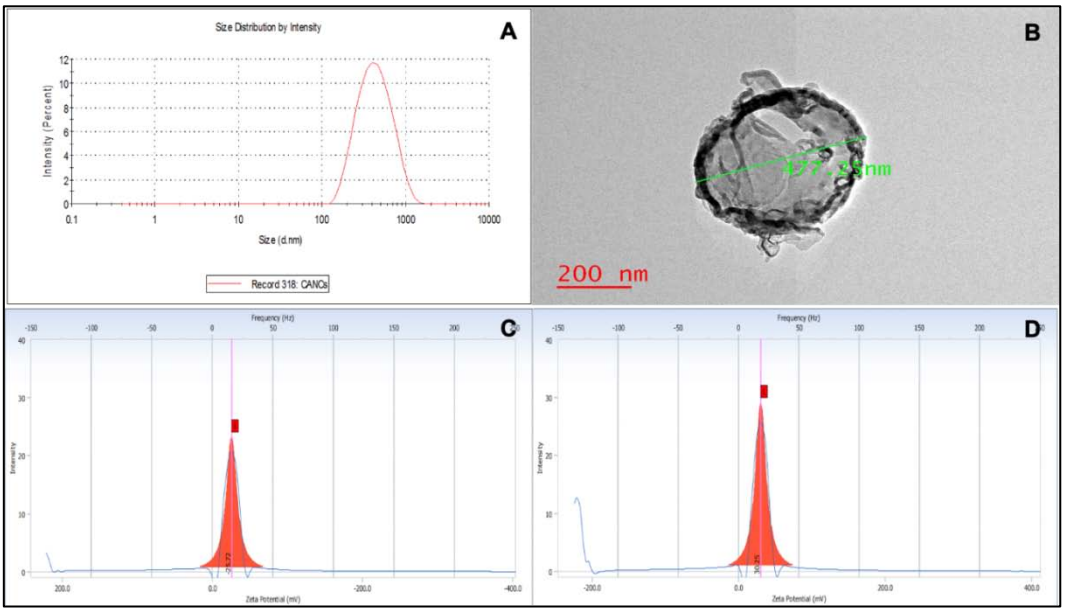

Fig. 4: Characterization of CANCs A. Graph for average particle size and particle size distribution obtained from DLS measurement, B TEM image of CANCs at 200 nm resolution, C Graph showing the zeta potential of the alginate nanocapsules before coating with Chitosan, D. Graph showing the zeta potential of the prepared CANCs

In vitro M-insulin release in response to glucose concentration was examined by placing CANCs within a dialysis bag. The dialysis bags containing CANCs were kept in a beaker with different glucose concentrations of 2.77 mmol/l, 5.5 mmol/l and 11.1 mmol/l, respectively at 37 °C under continuous stirring. The release of M-Insulin was also assessed in the absence of glucose i.e. in plain PBS pH 7.4. The CANCs did not displayed release of the M-Insulin in plain PBS pH 7.4 medium and in the medium with a glucose concentration of 2.77 mmol/l (Hypoglycemic level). However, an exponential increase in the release of M-insulin with an increase in glucose concentration from 5.5 mmol/l (Normoglycemic level) to 11.1 mmol/l (Hyperglycemic level) was observed (fig. 5). This might be attributed to the glucose concentration-dependent competitive binding of glucose with Con A and replacement of M-insulin. The increase in the release of the M-insulin into the medium was attributed to the swelling of the CANCs due to the diffusive movement of water molecules from the surrounding medium and the widening of the pores in the CANCs. It was found that approximately 58.0 % of the M-Insulin was released in the dialysing medium with high glucose concentration in 12 h.

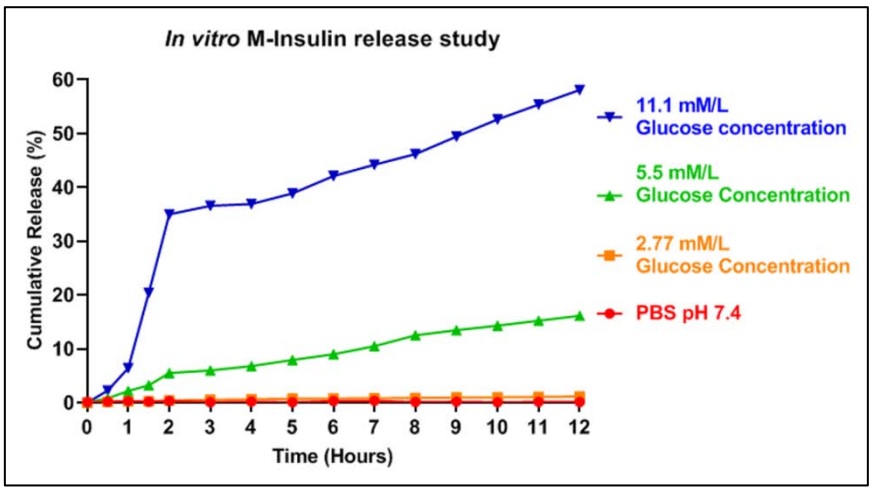

Fig. 5: *In vitro* M-insulin release study in mediums with different glucose concentrations

CONCLUSION

In conclusion, we report a novel platform for the glucose-responsive delivery of M-Insulin through nanocapsules. The formulation is designed to provide glucose affinity-driven replacement and self-regulated Maltose insulin delivery over a long period of time. The formulation was found to be effective in regulating the release of M-insulin for up to 12 h during *in vitro* studies and holds a great potential application for the glucose-responsive delivery of Insulin.

ACKNOWLEDGEMENT

The authors are thankful to the Department of Pharmaceutical Sciences, Dr. Harisingh Gour University, Sagar for providing infrastructure with sophisticated instrument facilities.

FUNDING

This work was supported by the Indian Council of Medical Research (ICMR), New Delhi, India (letter file no. 45/81/2018-NAN/BMS).

AUTHORS CONTRIBUTIONS

All the authors have contributed equally.

CONFLICTS OF INTERESTS

The authors report no conflict of interest

REFERENCES

1. Manorma, Mazumder R, Rani A, Budhori R, Kaushik A. Current measures against ophthalmic complications of diabetes mellitus-a short review. Int J App Pharm. 2021;13:54-65. doi: 10.22159/ijap.2021v13i6.42876.
2. Smith AG, Singleton JR. Diabetic neuropathy. Continuum (Minneap Minn). 2012;18(1):60-84. doi: 10.1212/01.CON.0000411568.34085.3e. PMID 22810070.
3. Suma S, Abeetha S, Divya R. Estimation of serum magnesium levels and its correlation among patients with diabetic retinopathy. Int J Pharm Pharm Sci. 2022 Oct 1:43-5.
4. Thorn LM, Forsblom C, Fagerudd J, Thomas MC, Pettersson Fernholm K, Saraheimo M. Metabolic syndrome in type 1 diabetes: association with diabetic nephropathy and glycemic control (the FinnDiane study). Diabetes Care. 2005;28(8):2019-24. doi: 10.2337/diacare.28.8.2019, PMID 16043748.
5. Schnell O, Cappuccio F, Genovese S, Standl E, Valensi P, Ceriello A. Type 1 diabetes and cardiovascular disease. Cardiovasc Diabetol. 2013;12(1):156. doi: 10.1186/1475-2840-12-156, PMID 24165454.
6. Federation ID. International diabetes federation: IDF diabetes atlas. Brussels, Belgium; 2019.
7. Federation ID. International diabetes federation: IDF diabetes atlas. Brussels, Belgium; 2021.
8. Bahman F, Greish K, Taurin S. Nanotechnology in insulin delivery for management of diabetes. Pharm Nanotechnol. 2019;7(2):113-28. doi: 10.2174/2211738507666190321110721. PMID 30907328.
9. Horvath K, Jeitler K, Berghold A, Ebrahim SH, Gratzer TW, Plank J. Long-acting insulin analogues versus NPH Insulin (human isophane insulin) for type 2 diabetes mellitus. Cochrane Database Syst Rev. 2007(2):CD005613. doi: 10.1002/14651858.CD005613.pub3, PMID 17443605.
10. Peterson GE. Intermediate and long-acting insulins: a review of NPH Insulin, insulin glargine and insulin detemir. Curr Med Res Opin. 2006 Dec 1;22(12):2613-9. doi: 10.1185/030079906X154178, PMID 17166343.
11. Siebenhofer A, Plank J, Berghold A, Narath M, Gfrerer R, Pieber T. Short acting insulin analogues versus regular human insulin in patients with diabetes mellitus. Cochrane Database Syst Rev. 2006 Apr 19;(2):CD003287. doi: 10.1002/14651858.CD003287.pub4
12. Rodrigues PA, Balan A, Purushothaman C. A prospective comparative observational study on safety, efficacy and cost-effectiveness of insulin and their analogues. Int J Pharm Pharm Sci. 2018 Jul 1;10(7):62. doi: 10.22159/ijpps.2018v10i7.21464.
13. Iwaoka H, Makino H, Yoshida S. Continuous subcutaneous insulin infusion. Nihon Rinsho. 1989;47(11):2577-82. PMID 2601069.
14. Ng SM, May JE, Emmerson AJ. Continuous insulin infusion in hyperglycaemic extremely low-birth-weight neonates. Biol Neonate. 2005;87(4):269-72. doi: 10.1159/000083863. PMID 15695923.
15. Pickup JC, Keen H, Parsons JA, Alberti KG. Continuous subcutaneous insulin infusion: an approach to achieving normoglycaemia. Br Med J. 1978;1(6107):204-7. doi: 10.1136/bmj.1.6107.204, PMID 340000.
16. Wisniewski N, Moussy F, Reichert WM. Characterization of implantable biosensor membrane biofouling. Fresenius J Anal Chem. 2000;366(6-7):611-21. doi: 10.1007/s002160051556, PMID 11225773.
17. Ma R, Shi L. Phenylboronic acid-based glucose-responsive polymeric nanoparticles: synthesis and applications in drug delivery. Polym Chem. 2014;5(5):1503-18. doi: 10.1039/C3PY01202F.
18. Vyas SP, Karajgi JS, Gogoi PJ, Jain NK. Development, characterization and evaluation of an auto-regulatory delivery system for insulin. J Microencapsul. 1991;8(2):235-42. doi: 10.3109/02652049109071491, PMID 1765903.
19. Volpatti LR, Matranga MA, Cortinas AB, Delcassian D, Daniel KB, Langer R. Glucose-responsive nanoparticles for rapid and extended self-regulated insulin delivery. ACS Nano. 2020 Jan 28;14(1):488-97. doi: 10.1021/acsnano.9b06395, PMID 31765558.
20. Gu Z, Dang TT, Ma M, Tang BC, Cheng H, Jiang S. Glucose-responsive microgels integrated with enzyme nanocapsules for closed-loop insulin delivery. ACS Nano. 2013;7(8):6758-66. doi: 10.1021/nn401617u, PMID 23834678.
21. Mody N, Sharma R, Vyas SP. Assessment of release kinetics of docetaxel loaded PLGA nanoparticles. Asian J Pharm Pharmacol. 2019 Jul;5(5):1031-7. doi: 10.31024/ajpp.2019.5.5.24.
22. United States Pharmacopeia. National formulary. Rockville, (MD): United States Pharmacopeial Commission; 2007.
23. Rani R, Kaur T, Singh AP, Singh AP. Formulation and evaluation of moronic acid-loaded transdermal patches. Int J Curr Pharm Sci 2021;13:81-8. doi: 10.22159/ijcpr.2021v13i6.1932.
24. Jain N, Verma A. Preformulation studies of pilocarpine hydrochloride as niosomal gels for ocular drug delivery. Asian J Pharm Clin Res. 2020 Apr 16:149-55. doi: 10.22159/ajpcr.2020.v13i6.37523.
25. Feldmeier HG, Rahn HW, Wolf I. Quantitative determination of crystallin insulin in insulin-zinc suspensions as an in-process control. Pharmazie. 1991 Jul 1;46(7):517-9. PMID 1784613.
26. Seo Young Jeong, Sung Wan Kimn, Eenink MJD, Feijen J. Self-regulating insulin delivery systems I. Synthesis and characterization of glycosylated insulin. J Control Release. 1984;1(1):57-66. doi: 10.1016/0168-3659(84)90021-X.
27. Gou Y, Geng J, Richards SJ, Burns J, Remzi Becer C, Haddleton DM. A detailed study on understanding glycopolymer library and con a interactions. J Polym Sci A Polym Chem. 2013;51(12):2588-97. doi: 10.1002/pola.26646, PMID 23761950.
28. Shen B, Yang S, Inventors. Composition and method for preparing alginate nanocapsules. United States Patent US. 2013 May 28;8(449):919.
29. Sarmento B, Ribeiro AJ, Veiga F, Ferreira DC, Neufeld RJ. Insulin-loaded nanoparticles are prepared by alginate ionotropic pre-gelation followed by chitosan polyelectrolyte complexation. J Nanosci Nanotechnol. 2007 Aug;7(8):2833-41. doi: 10.1166/jnn.2007.609, PMID 17685304.
30. El-Hussien D, El-Zaafarany GM, Nasr M, Sammour O. Chrysin nanocapsules with dual anti-glycemic and anti-hyperlipidemic effects: chemometric optimization, physicochemical characterization and pharmacodynamic assessment. Int J Pharm. 2021 Jan 5;592:120044. doi: 10.1016/j.ijpharm.2020.120044. PMID 33157212.
31. Kushwaha AK, Vuddanda PR, Karunanidhi P, Singh SK, Singh S. Development and evaluation of solid lipid nanoparticles of raloxifene hydrochloride for enhanced bioavailability. BioMed Res Int. 2013;2013:584549. doi: 10.1155/2013/584549. PMID 24228255.

32. Prusty AK, Sahu SK. Development and evaluation of insulin incorporated nanoparticles for oral administration. ISRN Nanotechnol. 2013 Jul 15;2013:1-6. doi: 10.1155/2013/591751.
33. Rahmawati R, Permana MG, Harison B, Yuliarto B, Kurniadi D. Optimization of frequency and stirring rate for synthesis of magnetite (Fe3O4) nanoparticles by using coprecipitation-ultrasonic irradiation methods. Procedia Eng. 2017:55-9.
34. Zohri M, Nomani A, Gazori T, Haririan I, Mirdamadi SS, Sadjadi SK. Characterization of chitosan/alginate self-assembled nanoparticles as a protein carrier. J Dispers Sci Technol. 2011 Apr;32(4):576-82. doi: 10.1080/01932691003757314.
35. Jelvehgari M, Barar J, Nokhodchi A, Shadrou S, Valizadeh H. Effects of process variables on micromeritic properties and drug release of non-degradable microparticles. Adv Pharm Bull. 2011;1(1):18-26. doi: 10.5681/apb.2011.003, PMID 24312752.